Metal–Organic Frameworks

DOI: 10.1002/ange.200602242

A Family of Nanoporous Materials Based on an Amino Acid Backbone**

*Ramanathan Vaidhyanathan, Darren Bradshaw, Jean-Noel Rebilly, Jorge P. Barrio, Jamie A. Gould, Neil G. Berry, and Matthew J. Rosseinsky**

Biological molecules interact with substrates with exquisite precision and (stereo)chemical selectivity, because of their ability to generate suitable receptor sites for substrate molecules. These sites have sufficient diversity in their bonding capabilities to allow subtle differentiation between molecular geometries. There is, thus, considerable interest in the preparation of synthetic materials with aspects of this function.[1] One approach is to use biologically derived components in the assembly of such materials. Amino acid residues are the origin for the functional properties and highly selective substrate-binding ability of many extended biological structures, and so are an attractive option as chiral building blocks for the preparation of bio-analogous materials. Herein, we report a family of synthetic crystalline nanoporous materials in which the internal surface is provided by the amino acid aspartic acid. These materials display enantioselective sorption that is strongly dependent on the spatial distribution of functional groups within the guest molecule.

Aspartic acid ($NH_2CH(COOH)CH_2COOH$, $aspH_2$) is an acidic amino acid with one amine and two carboxylic acid groups. As each of these functional groups is capable of binding to metal centers, the aspartate anion has a variety of coordination modes.[2] This polyfunctionality makes it a suitable organic node for the construction of porous metal–organic open-framework materials.[3–6] Extended frameworks based on metal aspartates have recently been reported;[2] however, the structural motifs in these frameworks are too dense to generate guest-accessible volume. The lactate[7] and tartrate[8] anions have also been used in the construction of metal–organic frameworks.

We have sought to generate porosity by connecting metal-aspartate units with suitable bidentate linker molecules. This objective requires a synthetic route that avoids the presence

[*] Dr. R. Vaidhyanathan, Dr. D. Bradshaw, Dr. J.-N. Rebilly, J. P. Barrio, J. A. Gould, Dr. N. G. Berry, Prof. M. J. Rosseinsky
Department of Chemistry
University of Liverpool
Liverpool, L69 7ZD (UK)
Fax: (+44) 151-794-3587
E-mail: m.j.rosseinsky@liv.ac.uk
Homepage: http://www.liv.ac.uk/Chemistry/Postgraduate/portfolio.html

[**] We thank the EPSRC for funding under EPSRC/C511794 and for access to the SRS, and the Leverhulme Trust for support of J.N.R.

Supporting information for this article is available on the WWW under http://www.angewandte.org or from the author.

of competing anions in the framework-forming step. This precaution is necessary to prevent structures that do not contain the amino acid from being templated by the counterion of the nickel source, and to prevent channel blockage by charge-balancing anions. The use of the preformed Ni(asp)·3 H_2O salt as a source of both cation and anion avoids this type of complication. Solvothermal reaction of Ni(L-asp)·3 H_2O with the bidentate aromatic nitrogen donor 4,4′-bipyridine (bipy) as the framework-forming linker in a water/methanol mixture at 150 °C affords the open-framework material [Ni_2(L-asp)$_2$(bipy)]·guests (**1**). Chiral gas chromatography (GC) confirms that the enantiopurity of the starting amino acid is delivered to the product by this route when either D- or L-aspartate is used as the starting material. Containing only one enantiomer of the amino acid, **1** adopts the chiral $P2_12_12$ space group, as indicated by the systematic absences in diffraction patterns produced by single crystals selected from the homochiral product.[18]

In **1**, neutral chiral Ni(L-asp) layers are connected by 4,4′-bipyridine linkers to afford a pillared structure with one-dimensional channels defined by the length of the 4,4′-bipyridine ligand and the separation between the nickel centers in the Ni(L-asp) layer (Figure 1 a). The chiral Ni(L-asp) layers are formed by octahedrally coordinated nickel centers linked by aspartate molecules, which each bind to one nickel center in a tridentate fac mode (by the amine and the α- and β-carboxylate groups) and to two other nickel centers in a monodentate mode (by the α- and β-carboxylate groups). The geometries of the resulting five- and six-membered chelate rings are comparable with those found in other materials featuring tridentate aspartate ligands.[9] The carboxylate groups each bridge two nickel centers in the syn–anti mode.

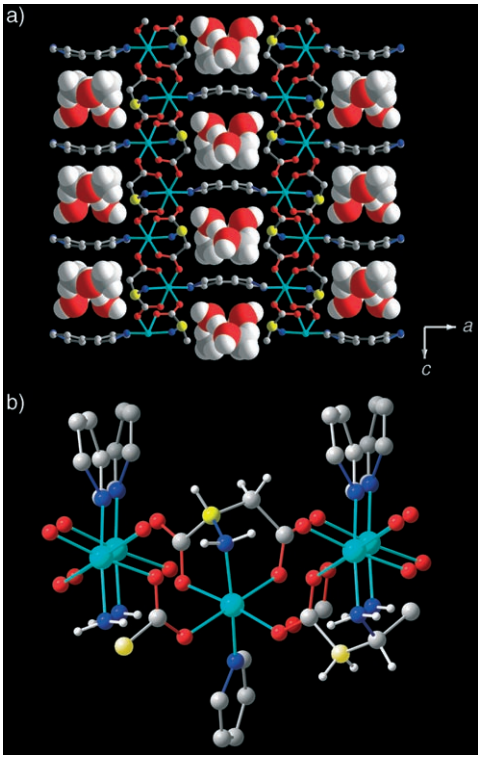

Figure 1. a) The connection of chiral Ni(L-asp) layers by 4,4′-bipyridine ligands produces framework **1**, which contains channels lined with amino acid residues. The disordered methanol and water guests that occupy the channels are represented with space-filling spheres. Hydrogen atoms and the minor disorder component of the 4,4′-bipyridine ligands are omitted for clarity. b) Part of the Ni(L-asp) layer of **1**, showing the coordination environments of the nickel centers. Ni cyan, C gray (chiral centers yellow), H white, N blue, O red.

In the octahedral coordination environment of the nickel cations, one triangular face comprises the amine nitrogen atom and oxygen atoms from both carboxylate functions of one aspartate molecule (Figure 1 b). The position trans to the amine group is occupied by a nitrogen atom from a 4,4′-bipyridine ligand. The two remaining coordination sites are occupied by oxygen atoms from carboxylate groups of two other aspartate molecules within the layer. Each nickel cation, thus, binds to three aspartate anions. The aspartate anions, in turn, link the metal center to four other nickel cations, which are coplanar and at a different height (along the *a* direction) to the central nickel cation, thus, imparting a corrugated nature to the layers. The tridentate aspartate anion links the nickel cation to two others by its two bridging carboxylate groups, while the two monodentate aspartate anions link the nickel cation to two further metal centers.

This corrugation requires that the 4,4′-bipyridine ligand bound to the central nickel cation and those bound to its four neighboring cations project outwards on opposite sides of the Ni(L-asp) layer. The distance (along the *c* direction) between the 4,4′-bipyridine pillars connecting two Ni(L-asp) layers is 7.73 Å, and the interlayer distance (along the *a* direction) between the nickel cations linked by the 4,4′-bipyridine molecules is 9.5 Å. The resulting channels (see Supporting Information), which run along the *b* direction, have a narrowest cross section of 3.8 × 4.7 Å (including van der Waals radii) and account for a solvent-accessible volume of 23.1 % of the total volume of **1**. The projection of the chiral carbon atoms of the aspartate units into the channels imparts chiral functionality to the internal surface of the material (Figure 1 b). In the as-prepared material, the channels are occupied by disordered water and methanol guest molecules (Figure 1 a). The composition of **1** refined from single-crystal X-ray diffraction data is [Ni_2(L-asp)$_2$(bipy)]·1.28 CH_3OH·0.72 H_2O.

Careful control over the water to methanol ratio is needed to achieve a homochiral material, as a competing achiral structure, [Ni_2(L,D-asp)$_2$(bipy)]·2 H_2O (**2**), forms by the racemization of the starting amino acid at higher water concentrations. Scanning electron microscope (SEM) images reveal considerable differences between the orthorhombic morphology of the chiral phase and the truncated polyhedral morphology of the racemic phase (see Supporting Information). The crystal structure of the racemic form **2** (space group $P2_1/n$) features similar Ni(asp) layers linked by 4,4′-bipyridine pillars, but successive layers are related by inversion symmetry.

The solvothermal synthesis based on Ni(L-asp)·3 H_2O is a generic route to a family of pillared open-framework materials with biologically derived internal surfaces. The replacement of 4,4′-bipyridine with related, but longer,

bridging nitrogen-donor ligands generates analogous materials with larger channels (see Supporting Information).

The phase purity of bulk **1** obtained from the solvothermal reaction between Ni(L-asp)·3 H_2O and 4,4′-bipyridine was established by powder X-ray diffraction (see Supporting Information). The phase purity is consistent with the homogeneous appearance of the material under SEM examination. Elemental analysis provided the composition $[Ni_2(L\text{-asp})_2(bipy)]\cdot CH_3OH\cdot H_2O$ (elemental analysis (%) calcd: C 38.96, H 4.13, N 9.56; found: C 38.94, H 4.11, N 9.64; inductively coupled plasma (ICP) analysis (%) calcd: Ni 20.04; found: Ni 20.12), which is in good agreement with the crystallographically derived formula.

The extended array of Ni–N and Ni–O bonds within the material confers thermal stability and robustness, such that **1** retains its open-framework structure upon loss of the methanol and water guest molecules from the channels. Thermogravimetric analysis of **1** under a nitrogen flow reveals a weight loss of 8.48% between room temperature and 200 °C (see Supporting Information), which is attributed to the removal of methanol and water molecules (calcd weight loss 8.55% from the analyzed composition). The similarity of the powder X-ray diffraction patterns of the as-prepared and the desolvated material demonstrates that the framework of **1** is stable to guest loss (see Supporting Information). The permanent porosity of **1** is demonstrated by the CO_2 sorption isotherm (see Supporting Information), from which a BET surface area of 247(3) $m^2 g^{-1}$ is obtained.

The detailed structural consequences of desolvation can be followed by single-crystal X-ray diffraction at 100 °C under a nitrogen flow (crystals of **1** remain stable and diffracting up to 200 °C). The desolvated crystal retains the framework structure of **1** (space group $P2_12_12$), but with no significant electron density in the channels.[18] Elemental analysis of the desolvated material corresponds to the composition $[Ni_2(L\text{-asp})_2(bipy)]$. The geometry of the Ni(L-asp) layers does not change markedly upon loss of the guests: the bond lengths and angles involving the nickel centers and the carbon, nitrogen, and oxygen atoms of the aspartate ligands are almost unchanged, within error, and the N-C-C-O torsion angle within the five-membered chelate ring remains 18.0(4)°.

Vapor sorption isotherms demonstrate that cyclohexane is not sorbed by **1**, placing an upper limit of 4.982 × 6.580 Å[10] on guest dimensions. Given the homochiral nature of the biologically derived internal surface of **1**, the extent of enantioselectivity possible in guest sorption is clearly of interest. We probed enantioselective sorption by using a library of small chiral molecules with closely related functionalities and found that there is a geometry-dependent interaction between the nanoporous material and the small-molecule guests. Table 1 lists the enantiomeric excess (*ee*) values found for the sorption of small chiral diols by **1** at 278 K, compared to those of the racemic standards. In all cases, the opposite enantiomer was enhanced by sorption when a host derived from D-aspartate, rather than L-aspartate, was used. The host samples were verified to be greater than 95% enantiopure before use in the tests; the use of host samples of lower enantiopurity reduced the observed *ee* value, in all cases.

Table 1: Sorption of chiral diols by **1** at 278 K.[a]

Diol	Extracted *ee* value[b]	Standard *ee* value[c]
1,2-propanediol	5.35	0.16
1,3-butanediol	17.93	0.62
1,2-butanediol	5.07	0.88
2,3-butanediol	1.5[d]	0.5
1,2-pentanediol	13.9[e]	0.34
2,4-pentanediol	24.5	0.00
2-methyl-2,4-pentanediol	53.77	0.46
2,5-hexanediol	3.4[f]	0.0
1,2-hexanediol	5	0.09

[a] The enantiomeric excess $ee = (R-S)/(R+S)*100$ was determined for the trifluoroacetic anhydride derivatives of the diols on a Lipodex-E capillary GC column (Machery Nagel). See Supporting Information for details. [b] For the guest diols recovered by distillation from **1**, after exposure of **1** to the liquid diol for 16 h. [c] For the racemic diol standard. [d] Extracted 71.4% meso; standard 65.7% meso. [e] Extracted 45.1% meso; standard 50.7% meso. [f] Extracted 58.5% meso; standard 53.6% meso.

The levels of enantioselection for the sorption of these small molecules are significant, but it is the differentiation between diols with similar chain lengths but differing separations between the hydroxyl groups which is particularly striking. Considering a fixed chain length of four carbon atoms, 1,2-butanediol and 2,3-butanediol display considerably reduced enantioselection relative to 1,3-butanediol. The favorable nature of the 1,3-disposition of the diol units is further demonstrated by the high *ee* value of 2,4-pentanediol, in comparison with those of 1,2-pentanediol and 2,5-hexanediol. The highest sorption *ee* value observed within the library of diol guests studied was 53.7% for 2-methyl-2,4-pentanediol, a monosubstituted derivative of 2,4-pentanediol with only one chiral center.

The characteristics of the interactions between a diol guest and the internal surface of a porous material composed of Ni(asp) layers and 4,4′-bipyridine pillars are revealed by the crystal structure of $[Ni_2(L,D\text{-asp})_2(bipy)]\cdot CH_2(OH)CH(OH)CH_3$ (**3**),[18] which was prepared solvothermally in 1,2-propanediol. The framework of **3** adopts the racemic structure of **2**, as the conditions required to grow crystals of suitable size and quality from the diol solvent result in the racemization of the aspartate anion. However, given the similarity in structure between **1** and **2**, the structure of **3** can serve as a model for the guest binding motifs in the chiral host **1** as well. In the refined structure of **3**, the guest is located in a pocket defined by two neighboring 4,4′-bipyridine molecules and adopts an extended conformation, with the diol groups hydrogen bonded to the oxygen atoms of β-carboxylate groups in two Ni(asp) layers (Figure 2).

It was not possible to grow analogues of **1** with chiral guests; therefore, we used computational approaches to identify different modes of interaction between the guests and **1** that might explain the pronounced differences in enantioseparation. The efficient center-of-mass and conformational searching of a docking routine based on molecular mechanics was combined with higher-level quantum-mechanical calculations (see Supporting Information). Such docking

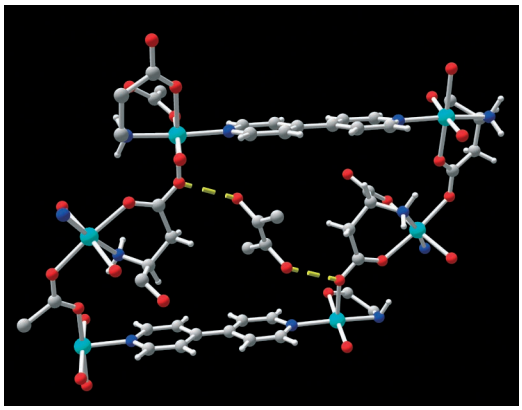

Figure 2. Location of 1,2-propanediol within the channels of **3**. As the 1,2-propanediol molecule is disordered over a crystallographic inversion center, each of the methyl groups shown has an occupancy of 50%; further disorder involving the methyl groups is omitted for clarity. Hydrogen bonds are represented by dashed yellow lines. Ni cyan, C gray, H white, N blue, O red.

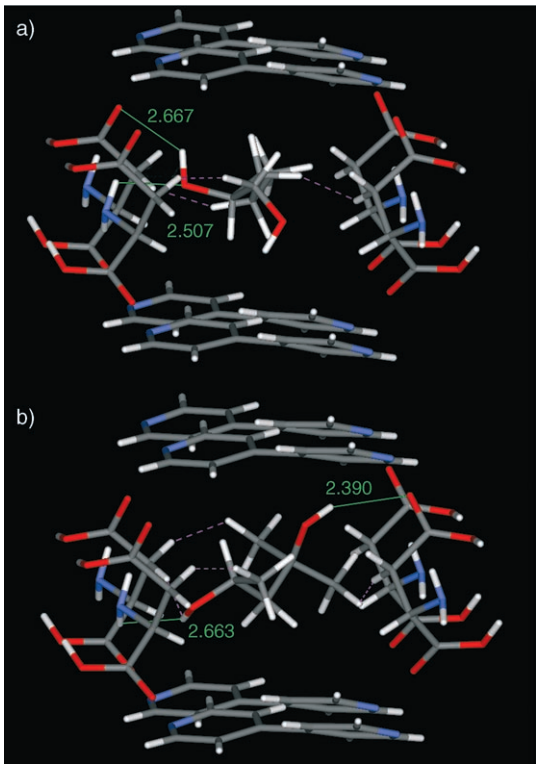

Figure 3. Location of a) (*S*)-1,2-pentanediol and b) (*S*)-2-methyl-2,4-pentanediol within the channels of **1**, as determined by the combination of molecular-mechanics docking and semi-empirical quantum-mechanical optimization. Hydrogen bonds are represented by solid green lines; potentially unfavorable contacts (with distances of less than 84% of the sums of the van der Waals radii) are represented by dashed pink lines. C gray, H white, N blue, O red; Ni atoms are omitted.

approaches have been extensively validated in the study of drug–receptor interactions in proteins and other biomolecules[11,12] and involve genetic-algorithm-driven searches of the conformational and positional space of guest species. These methods were tested by successfully reproducing the location of the 1,2-propanediol guest in **3**. The docking procedure was then applied to the interaction of **1** with the two guest molecules 1,2-pentanediol (13.9% *ee*, Table 1) and 2-methyl-2,4-pentanediol (53.77% *ee*, Table 1). These guests were chosen to investigate the factors responsible for enantioselection, as they have alkyl backbones of the same length. However, the *ee* values observed indicate that the differential free energy of sorption of enantiomers of the two guests differ by a factor of four. The molecular-mechanics docking procedures indicated differing modes of interaction for the 2-methyl-2,4-pentanediol and 1,2-pentanediol guests with the framework. The most popular docked pose of each enantiomer of the guests was then optimized within the framework using semi-empirical quantum-mechanical calculations at the PM3 level; this quantum mechanical optimization did not greatly change the geometry or location of the guest (the largest root-mean-square deviation between the docked and PM3-optimized structures was 0.68 Å).

As expected, given their equal alkyl-chain lengths, both 2-methyl-2,4-pentanediol and 1,2-pentanediol sit in essentially identical sorption sites within the framework of **1** (Figure 3). The guest pocket is defined by two aspartate residues on opposite sides of the channel and by two 4,4′-bipyridine molecules on opposite sides of the channel. However, within this pocket, the two guests interact in different ways with the framework. The approach geometries are similar for both enantiomers in each case (for example, the difference between the sorption energies of the enantiomers of 2-methyl-2,4-pentanediol is 2.8 kJ mol^{-1}). As the small differences between the interactions of the enantiomers of each guest cannot be reliably addressed by the present calculations, we instead use the calculations to identify the different modes of interaction of the two guests (*S* enantiomers) with the framework. The secondary alcohol group of (*S*)-1,2-pentanediol interacts with the framework of **1** by hydrogen bonding with the β-carboxylate group of an aspartate residue (OH···O 2.667 Å) and the amine group of another aspartate residue (O···HN 2.507 Å). The primary alcohol group is located at the center of the channel and does not hydrogen bond to the framework (Figure 3a). In contrast, both alcohol groups of (*S*)-2-methyl-2,4-pentanediol (which is sorbed by **1** with a higher *ee* value) participate in hydrogen bonds with the framework (Figure 3b). The tertiary alcohol group forms hydrogen bonds with the β-carboxylate group of an aspartate residue (OH···O 2.390 Å), and the secondary alcohol group forms a hydrogen bond with the amine group of another aspartate residue (O···HN 2.663 Å). The very different modes of interaction of the two guest molecules may produce the observed differences in enantioselection. The differentiation of substrates on the basis of multiple interactions within a compositionally complex pocket is reminiscent of the selective function of enzymes.

The dimensions of the channels in this amino acid derived open-framework material are on the order of those found in zeolites, but are smaller than the largest found in metal–organic frameworks (of nm-scale diameter).[13,14] For molecular recognition applications, such as chiral sorption, a good match of size and shape between the desired guest and the

host is important; large-pore homochiral frameworks cannot separate small-molecule guests in this way.[15] This observation demonstrates that not only channel size, but also channel surface chemistry is important for functional behavior in metal–organic frameworks. The preparation of frameworks with internal surfaces derived from amino acids opens up the possibility of new classes of nanoporous materials for chiral catalysis and sorption,[16,17] and will enhance efforts to establish and understand solid-state geometries for bio-analogous recognition behavior.

Experimental Section

Experimental details are given in the Supporting Information.

Received: June 5, 2006
Published online: September 7, 2006

Keywords: amino acids · chirality · metal–organic frameworks · nanoporous materials · sorption

[1] M. Yoshizawa, M. Tamura, M. Fujita, *Science* **2006**, *312*, 251.
[2] E. V. Anokhina, A. J. Jacobson, *J. Am. Chem. Soc.* **2004**, *126*, 3044.
[3] B. F. Abrahams, B. F. Hoskins, D. M. Michail, R. Robson, *Nature* **1994**, *369*, 727.
[4] O. M. Yaghi, M. O'Keeffe, N. W. Ockwig, H. K. Chae, M. Eddaoudi, J. Kim, *Nature* **2003**, *423*, 705.
[5] N. Guillou, C. Livage, M. Drillon, G. Férey, *Angew. Chem.* **2003**, *115*, 5472; *Angew. Chem. Int. Ed.* **2003**, *42*, 5314.
[6] R. Matsuda. R. Kitaura, S. Kitagawa, Y. Kubota, R. V. Belosludov, T. C. Kobayashi, H. Sakamoto, T. Chiba, M. Takata, Y. Kawazoe, Y. Mita, *Nature* **2005**, *436*, 238.
[7] D. N. Dybtsev, A. L. Nuzhdin, H. Chun, K. P. Bryliakov, E. P. Talsi, V. P. Fedin, K. Kim, *Angew. Chem.* **2006**, *118*, 930; *Angew. Chem. Int. Ed.* **2006**, *45*, 916.
[8] S. Thushari, J. A. K. Cha, H. H.-Y. Sung, S. S.-Y. Chui, A. L.-F. Leung, Y.-F. Yen, I. D. Williams, *Chem. Commun.* **2005**, 5515.
[9] L. P. Battaglia, A. Bonamartini Corradi, L. Antolini, G. Marcotrigiano, L. Menabue, G. C. Pellacani, *J. Am. Chem. Soc.* **1982**, *104*, 2407.
[10] C. E. Webster, R. S. Drago, M. C. Zerner, *J. Am. Chem. Soc.* **1998**, *120*, 5509.
[11] C. Hetényi, D. V. D. Spoel, *Protein Sci.* **2002**, *11*, 1729.
[12] G. M. Morris, D. S. Goodsell, R. S. Halliday, R. Huey, W. E. Hart, R. K. Belew, A. J. Olson, *J. Comput. Chem.* **1998**, *19*, 1639.
[13] G. Férey, C. Mellot-Draznieks, C. Serre, F. Millange, J. Dutour, S. Surblé, I. Margiolaki, *Science* **2005**, *309*, 2040.
[14] H. K. Chae, D. Y. Siberio-Pérez, J. Kim, Y.-B. Go, M. Eddaoudi, A. J. Matzger, M. O'Keeffe, O. M. Yaghi, *Nature* **2004**, *427*, 523.
[15] D. Bradshaw, T. J. Prior, E. J. Cussen, J. B. Claridge, M. J. Rosseinsky, *J. Am. Chem. Soc.* **2004**, *126*, 6106.
[16] C.-D. Wu, A. Hu, L. Zhang, W. Lin, *J. Am. Chem. Soc.* **2005**, *127*, 8940.
[17] J. S. Seo, D. Whang, H. Lee, S. I. Jun, J. Oh, Y. J. Jeon, K. Kim, *Nature* **2000**, *404*, 982.
[18] Crystallographic data for solvated **1** ($[Ni_2(L\text{-asp})_2(bipy)]\cdot 1.28\,CH_3OH\cdot 0.72\,H_2O$): $C_{19.28}H_{24.56}N_4Ni_2O_{10}$, $M_r = 589.84$, orthorhombic, space group $P2_12_12$, $a = 22.2721(13)$, $b = 6.8371(4)$, $c = 7.7308(5)$ Å, $V = 1177.22(12)$ Å^3, $Z = 2$, $\lambda = 0.84600$ Å, $T = 150(2)$ K, $R_1 = 0.0432$, $R_w = 0.1128$. For desolvated **1** ($[Ni_2(L\text{-asp})_2(bipy)]$): $C_{18}H_{18}N_4Ni_2O_8$, $M_r = 535.78$, orthorhombic, space group $P2_12_12$, $a = 22.245(2)$, $b = 6.7907(7)$, $c = 7.7387(8)$ Å, $V = 1169.0(2)$ Å^3, $Z = 2$, $\lambda = 0.84600$ Å, $T = 373(2)$ K, $R_1 = 0.0350$, $R_w = 0.0809$. For **3** ($[Ni_2(L,D\text{-asp})_2(bipy)]\cdot CH_2(OH)CH(OH)CH_3$): $C_{21}H_{26}N_4Ni_2O_{10}$, $M_r = 611.87$, monoclinic, space group $P2_1/n$, $a = 6.5697(4)$, $b = 22.6167(13)$, $c = 7.8511(5)$ Å, $\beta = 90.1540(10)°$, $V = 1166.55(12)$ Å^3, $Z = 2$, $\lambda = 0.67270$ Å, $T = 100(2)$ K, $R_1 = 0.0390$, $R_w = 0.0950$. CCDC-607296 (solvated **1**, 150 K), CCDC-607297 (desolvated **1**, 373 K), and CCDC-607295 (**3**) contain the supplementary crystallographic data for this paper. These data can be obtained free of charge from The Cambridge Crystallographic Data Centre via www.ccdc.cam.ac.uk/data_request/cif.

